Structural robustness at the conceptual stage

Aurélie Deschuyteneer, Denis Zastavni

LOCI, Université catholique de Louvain, Louvain-la-Neuve, Belgium

Contact: aurelie.deschuyteneer@uclouvain.be

Abstract

The aim of this paper is to develop a complementary method to the numerical approaches proposed in the literature on the subject, which will help in assessing the constitutive dimensions of structural robustness at the conceptual stage. Based on geometrical thinking, this method defines robustness as the ability of a structure to maximise the rearrangement of its internal forces. This can be expressed graphically by admissible geometrical domains. The purpose and extent of this new approach are summarised and illustrated by the detailed robustness analysis of two case studies. The areas obtained for the admissible geometrical domains are then compared with values of the minimal load path and with structural stiffness, in order to decide on the right modelling strategy.

Keywords: robustness; structural design; strut-and-tie modelling; force redistributions; geometrical approach

1 Introduction

Structural robustness is a concept that started to be used after the 1968 incident at Ronan Point tower block, near London, where a gas explosion led to the entire collapse of a corner of the building.

Requirements linked to structural robustness are detailed in several different ways in literature on the subject. The definition made by Knoll and Vogel, for example, assesses robustness as "*the property of systems that enables them to survive unforeseen or unusual circumstances*" [1]. Such a definition proposes a good conceptual approach to the required performance, as long as it remains qualitative. However, when it comes to characterise a structure in particular, the lack of quantitative approaches can make the distinction between what is robust and what is not difficult. This can be problematic as robustness is a property required by design laws [2] [3], which should then be absolute – objective, universal and based on independent indices.

In practice, we can note that numerous structures nowadays are still prone to collapse through a deficit of robustness, even if they have been extensively verified by structural engineers [4]. Indeed, these verifications (reviewed in section 2), based on numerical approaches, can only assess robustness for chosen failure scenarios in structures that have already been designed. This, of course, does not allow coverage of the total range of possible unexpected damage that may occur during the life of a structure.

The aim of this paper is to develop a new complementary approach to structural robustness, based on geometrical thinking. This will allow taking robustness into account at the conceptual stage, and so at the very first step of the design process. In this perspective, robustness is defined as the property of structures that allows for maximisation of the rearrangement of their internal forces.

Section 2 will first review the existing numerical approaches to structural robustness and their limitations for the problem under consideration.

Section 3 details the concept of admissible geometrical domain, which serves as the indicator of robustness for the proposed approach. Two case studies, presented in Sections 4 and 5, then compare the geometrical results with load paths and stiffness analyses. This shows how admissible geometrical domains can orient structural design towards optimal robustness solutions.

2 Structural robustness in literature

Several approaches to assess structural robustness numerically can be found in literature on the subject. These can be organised into four major types: probabilistic, risk-based, deterministic and energetic [4].

2.1 Probabilistic approaches

The probability *P(f)* of progressive collapse, which is caused when a local failure in a building triggers damage disproportionate to the original cause, is detailed by Val and Val [5] as:

$$P(f) = P(f/DA_i)\,P(D/A_i)\,P(A_i) \qquad (1)$$

where $P(A_i)$ is the probability of the occurrence of an accidental event A_i, $P(D/A_i)$ is the probability of local damage given the occurrence of A_i, and $P(f/DA_i)$ is the probability of progressive collapse given the occurrence of D due to A_i.

2.2 Risk-based approaches

An index of robustness I_{Rob} is proposed by Baker et al. [6], which measures the fraction of total system risk resulting from direct consequences:

$$I_{Rob} = R_{Dir} \,/\, (R_{Dir} - R_{Ind}) \qquad (2)$$

where R_{Dir} is the risk of failure caused by local damage, and R_{Ind} is the risk of indirect consequences due to this local damage.

2.3 Deterministic approaches

Based on the *Residual Influence Factor* used in the offshore industry, the Frangopol and Curley strength redundant factor is defined as [7]:

$$R = L_{Intact} \,/\, (L_{intact} - L_{damaged}) \qquad (3)$$

where L_{intact} is the load carrying capacity of the intact structure, and $L_{damaged}$ the load carrying capacity of the damaged structure according to determined failure scenarios.

2.4 Energetic approaches

Energetic approaches consist in evaluating the work of failure (or deformation energy) of a structure, by integrating the area under its force-displacement curve up to collapse [8].

The aim of these four types of approaches is to characterize robustness by a numerical analysis of the capacities of resistance - or possibly of redistribution - of a structure. This is done once the structural design has been fixed, which makes these approaches inconvenient when it comes to interacting with the design and the related robustness performance. The following section details a fifth approach to assess robustness, which answers this lack. This method, further detailed in [9], has also been calibrated by a comparative analysis with the results found via the deterministic and energetic approaches.

3 Proposed geometrical approach

3.1 Graphic Statics

The proposed geometrical approach is based on Graphic Statics, which was the method used for structural analysis for most of the 20th century. Formalised in the 19th century by Maxwell [10], it builds on two reciprocal diagrams (Figure 1):

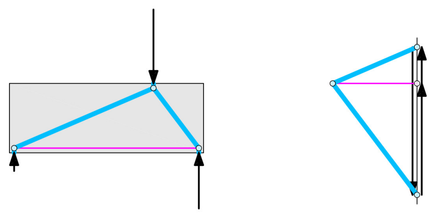

Figure 1. Form diagram (left) and force diagram (right)

- a form diagram, which gives the structural geometry and the load paths;
- a force diagram, which gives the force equilibrium of each node of the structure. Force intensity is also given by a simple measure of their respective lengths in the diagram, without any calculation.

For all the figures, paths in compression (struts) are depicted in bold and blue, while paths in tension (ties) are shown by thin and magenta lines.

As detailed by Zalewski & Allen [11], Graphic Statics still reveals itself today to be an efficient method for structural design. It is indeed a simple method, based on drafting tools only, and can be used to design a wide range of structures. Besides it supplies real-time information about geometry and efforts that are linked to it, it also allows manipulating design parameters very easily.

3.2 Admissible geometrical domains

Graphic Statics has recently been extended by Fivet [12], to include useful and necessary operations during structural design. Fivet developed an interactive IT tool, which includes a set of geometric constraints that can be applied on the nodes of the form and force diagrams of a given structure. These guarantee that:

- static equilibrium is ensured, which is a necessary preliminary condition;
- boundary conditions are respected (geometric criterion);
- maximum admissible constraints in the material are not exceeded (resistance criterion). A rigid-plastic behaviour has been considered, and compatibility of deformations neglected.

The set of positions a node can take in order to respect these three constraints is called its admissible geometrical domain. Figure 2 illustrates the admissible geometrical domain for the magenta point of the force diagram. Its linear borders represent the geometric criterion, while the circular borders set the resistance criterion.

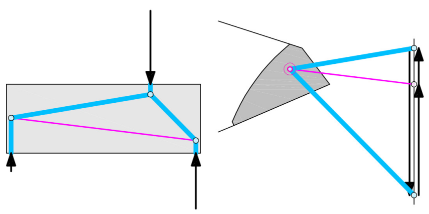

Figure 2. Admissible geometrical domain of the magenta point

The admissible geometrical domain is taken as a robustness indicator by the present approach. A larger domain will indeed allow more admissible positions for the point it is linked to, and hence a greater aptitude for plastic redistribution of forces in the structure.

3.3 Parameters influencing robustness

The two criteria of geometry and resistance that allow constructing the admissible geometrical domain can be correlated to two of the sixteen parameters defined by Knoll and Vogel as being constitutive of the performance of robustness [1]:

- multiple load paths or redundancy, which assesses that several load paths can be mobilized initially in a structure. If one is disabled due to damage, the others can continue to carry the applied loads under certain conditions;
- strength, through supplementary resistance provided to the structure.

These two parameters can easily be implemented at the conceptual stage within the proposed geometrical approach. The resulting admissible geometrical domain shows in effect what the consequences are of design manipulations on the ability to redistribute forces. In this point of view, the method tends to complete the existing numerical approaches which are more focused on structural analysis. Another advantage is the possibility to interact with the design, promoted by the immediate and visual results provided by the geometric indicator. This allows efficiently designing for robustness, in addition to assessing it.

The two next sections will illustrate the concept of admissible geometrical domain through case studies. These domains will also be compared with the concept of load paths and with stiffness criteria obtained via elastic analyses.

4 Case studies

4.1 Concrete wall with one opening

This first case study is based on a canonical example developed by Schlaich, Schäfer and Jennewein [13]. It consists in a concrete shear wall, supported at both extremities, the design compression strength of which is 17 [MPa] (this corresponds to C25/30 concrete). As in [13], the wall is 7 [m] long, 4.7 [m] high and 0.4 [m] thick, and has a 1.5x1.5 [m] opening in the bottom left corner. The 25 [cm] cover considered is represented by the dotted lines in the figures. The aim is to define possible reinforcement layouts (in BE 500 S steel) to allow a 3 [MN] punctual vertical force to act on the top of the wall at approximately 3/5 of its length (Figure 3).

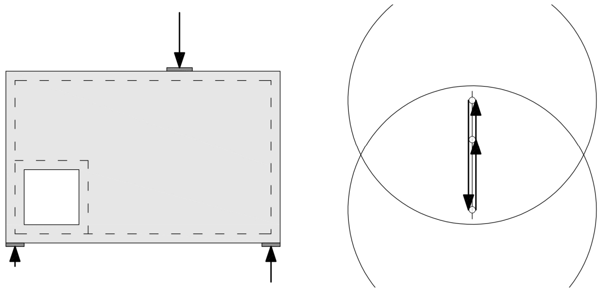

Figure 3. Case study 1

Several methods have been considered to model the structural behaviour of concrete, in order to compare them and validate the proposed geometrical approach for assessing robustness.

4.1.1 Elastic stresses

Elastic stresses in the wall have first been analysed using some of the applets [14] available on the website of the iBeton lab of the *École Polytechnique Fédérale de Lausanne*. The iMesh applet allows one to model the structure, while iConc performs a linear elastic analysis (Figure 4). Blue lines represent elastic stresses in compression while the red lines are in tension, lengths being proportional to the intensity of stresses.

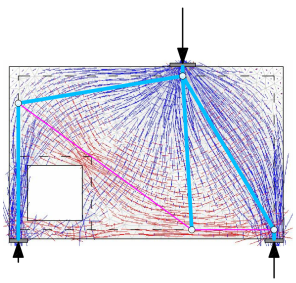

Figure 4. Elastic stresses and two-ties network

4.1.2 Admissible geometrical domains

Adapted and extended from [13], different strut-and-tie networks can be drawn inside the structure: a funicular (Figure 5), a catenary (Figure 6), a two-ties (Figure 7) and a truss (Figure 8). This represents a correct conceptual abstraction of the inner stress fields because buckling and anchoring forces between struts and ties are here neglected.

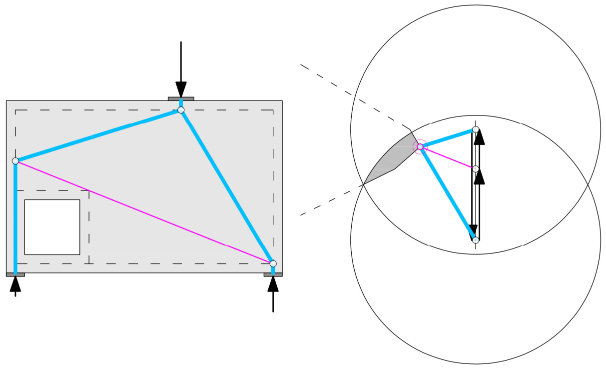

Figure 5. Funicular network

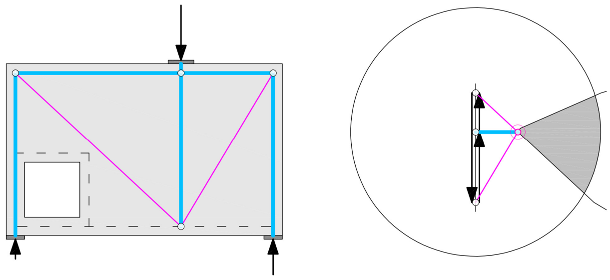

Figure 6. Catenary network (with continuous upper strut, and vertical strut with a fixed orientation)

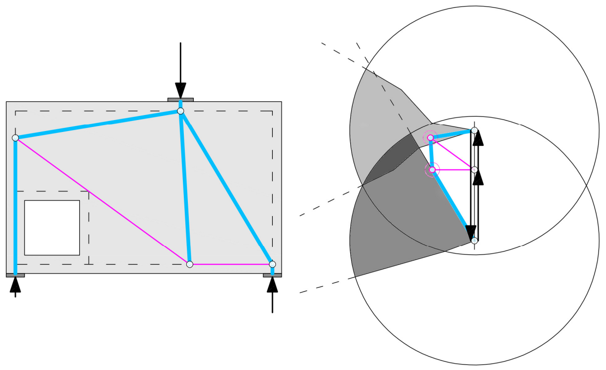

Figure 7. two-ties network

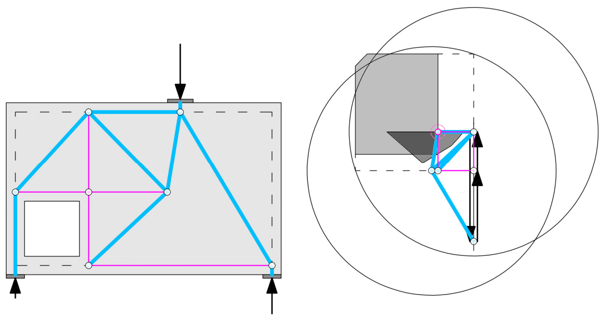

Figure 8. Truss network (for ties with a fixed orientation)

For these four networks, the admissible geometrical domains are built for the magenta point(s) of the force diagram. Linear borders ensure that forces stay inside the chosen geometry and its 25 [cm] cover. Circular borders set the maximum forces in concrete, their radius being:

$$0.4\ [m]\ x\ 0.5\ [m]\ x\ 17\ [MPa] = 3.4\ [MN] \quad (4)$$

Areas of these domains, expressed in [MN²] as the force diagram represents forces in [MN], are given in the first column of Table 1. When three values are proposed, the first corresponds to the domain of the upper magenta point, the second to the lower, and the third to the total domain. For the truss network depicted here, the two magenta points are superimposed. Note also that, for the two-ties network, domain intersection gives the same area as those of the funicular network.

Table 1. Results of the analyses

	A [MN²]	T - C [MNm]	T + C [MNm]	k [MN/m]
Funicular (Figure 5)	0.712	-14.10	38.57	272.72
Catenary (Figure 6)	3.261	-14.10	55.37	250.00
Two-ties (Figure 7)	4.864 7.792 **11.943**	-14.10	**36.69**	**375.00**
Truss (Figure 8)	6.122 0.962 6.445	-14.10	42.66	300.00

As we can expect that robustness increases with the size of the admissible geometrical domain, it is thus the two-ties network that presents the best performance regarding allowable force redistributions. Moreover, as evidenced in Figure 4, this network proposes a strut-and-tie configuration very close to the path of elastic stresses.

4.1.3 Load paths

Maxwell's theorem, reformulated by Baker et al in [15], allows the characterization of truss layouts via two equations. *L* corresponds to the length of the bars, measured in the form diagram; *F* is the length of the bars, measured in the force diagram; *V* is the volume of material; and *σ* is the maximum admissible stress in the material. *T* indices correspond to forces in tension, while *C*'s correspond to compression. These equations are:

$$\Sigma L_T F_T - \Sigma L_C F_C = \Sigma V_T \sigma_T - \Sigma V_C \sigma_C \\ = \Sigma \vec{F_i} \bullet \vec{r_i} = constant\ = T - C \quad (5)$$

which gives the negative of the work required by the applied loads to cancel out the reactions, this value remaining constant as long as the intensity and position of the applied forces and location of supports do not change, and:

$$\Sigma L_T F_T + \Sigma L_C F_C = \Sigma V_T \sigma_T + \Sigma V_C \sigma_C \\ = \sigma V_{tot}\ = T + C \quad (6)$$

which gives a value proportional to the total required volume for the members, considering that the maximum allowable stress in tension equals those in compression. For a given structure, this means finding the strut-and-tie network that leads to the minimal volume of material. Considering efficiency, this network is called "optimal load path".

When applying these equations to the case study, the minimal load path is calculated for every strut-and-tie network to help selecting the right structural behaviour. This is done by finding the optimal position of the different magenta points inside their admissible domain, which are the ones illustrated in Figures 5 to 8. The results of equations (5) and (6) are given in the second and third column of Table 1 respectively. Equation (5) is verified for all the models, as *T-C* remains constant. For equation (6), the minimal value of *T+C* will be reached for the optimal load path of the two-ties network.

4.1.4 Stiffness considerations

In order to define which structural behaviour will be primarily activated, the four networks are then analysed with classical mechanical software to obtain their respective stiffness, defined as:

$$k\ [MN/m] = F\ [MN]/d\ [m] \quad (7)$$

with *F* the applied load and *d* the maximum displacement of the points of the network. The obtained values, set out in the last column of Table 1, show that the two-ties network will be the stiffest. Stiffness is obtained for steel ties dimensioned to sustain a maximum effort of 3.4 [MN], as in concrete. This corresponds to a rebar section of 78.34 [cm²]. Local degrees of cracking in concrete have not been taken into consideration for this stiffness assessment.

4.1.5 Comparison of results (Table 1)

Comparison of results meets the observation of [15], which states that the optimal network - the two-ties one - is the lightest and the stiffest at the same time. It is also the network which is linked to the largest admissible geometrical domain.

In their paper, Schlaich & al. [14] concluded that both of the networks they considered - a two-ties one and more complex truss - would carry half the applied load. Stiffness analyses here performed reveal that the two-ties network is stiffer than the truss, thus it will carry a greater proportion of the applied load. Moreover, values obtained via the other types of analyses show that these two models are not equivalent, the two-ties network always presenting better performances.

The same type of analyses will now be performed for a more complex case study.

4.2 Concrete wall with two openings

The second case study is inspired by those analysed in Section 4.1. but has been made more complex, with the bottom opening turned into a door and another square opening added on the top right corner of the wall (Figure 9). The wall is 10 [m] long, 10 [m] high and 50 [cm] thick. The 3 [m] wide and 5 [m] high door is located at 1 [m] of the left extremity of the wall. The 3 by 3 [m] window is located at 1 [m] of the upper extremity of the wall and 2 [m] from its right edge. Forces between 125 and 237.5 [kN] are acting on the top of the structure. Here a C30/37 concrete has been considered, with a 10 [cm] cover.

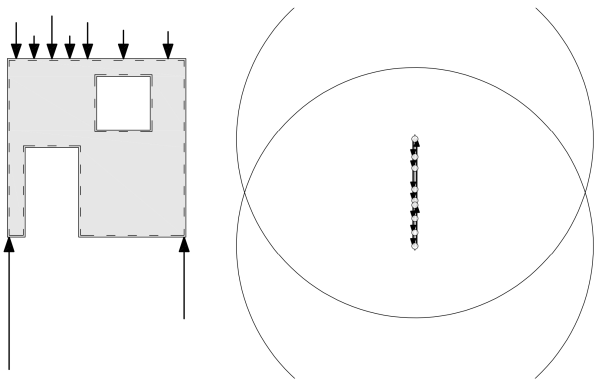

Figure 9. Case study 2

4.2.1 Elastic stresses

The same analysis as in Section 4.1.1. is performed on the second study case (Figure 10):

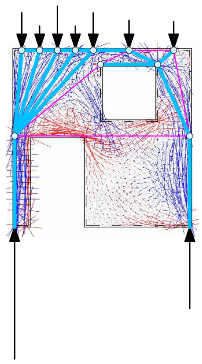

Figure 10. Elastic stresses and fan-like network

4.2.2 Admissible geometrical domains

Five types of strut-and-tie networks are now analysed: two funicular types (Figures 11 & 12), a catenary (Figure 13), a fan-like (Figure 14) and a truss (Figure 15). The depicted domains show the allowable orientations of the lowest tie, represented in the force diagram by the magenta point. The radius of the circles setting the maximum admissible stress in concrete is:

$$0.5\ [m]\ x\ 0.2\ [m]\ x\ \frac{30\ [MPa]}{1.5} = 2\ [MN] \qquad (8)$$

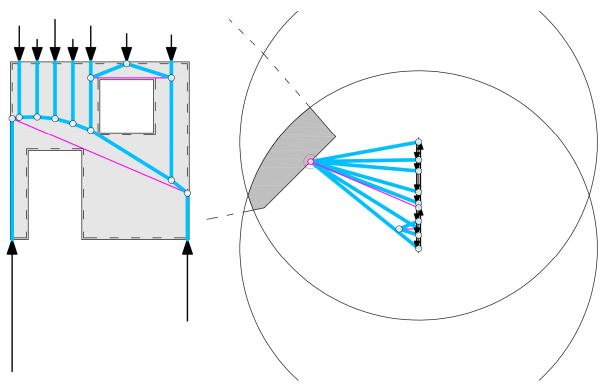

Figure 11. First funicular network

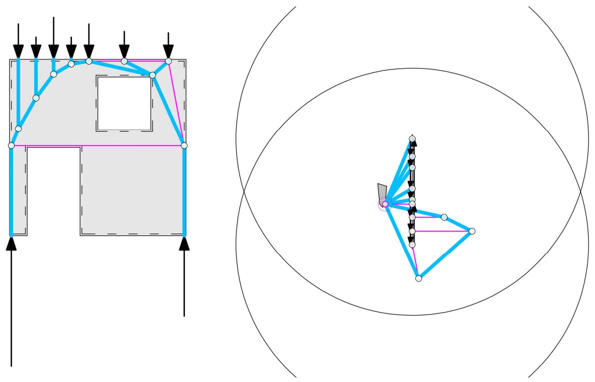

Figure 12. Second funicular network

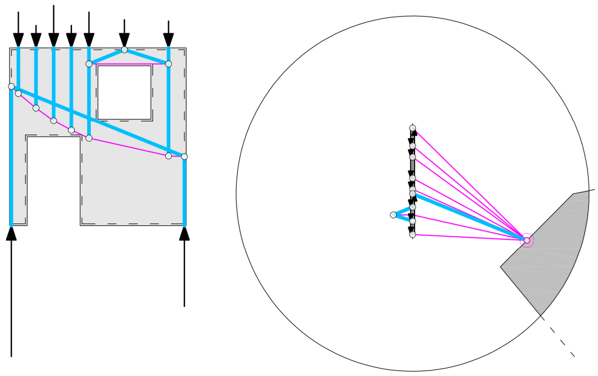

Figure 13. Catenary network

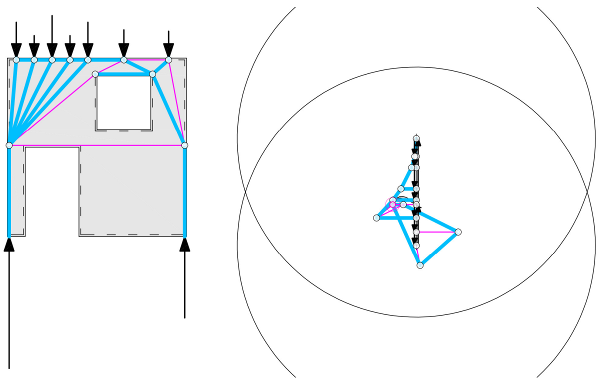

Figure 14. Fan-like network

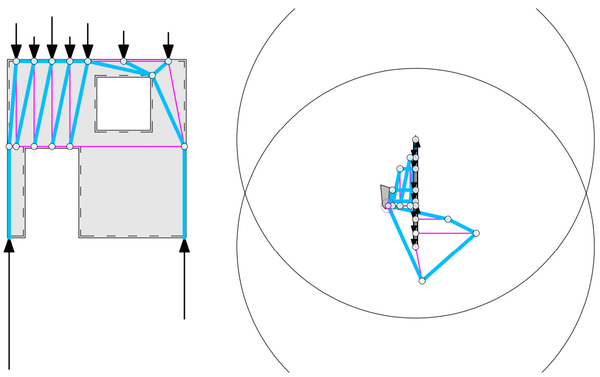

Figure 15. Truss network (with continuous lower tie)

The area of these domains, expressed in [MN²], is given in the first column of Table 2. Thus it is the catenary network that presents the best robustness properties when considering the size of the admissible geometrical domain. Moreover, as evidenced in Figure 10, this network proposes a strut-and-tie configuration very close to the path of elastic stresses.

Table 2. Results of the analyses

	A [MN²]	T - C [MNm]	T + C [MNm]	k [MN/m]
Funicular 1 (Figure 11)	0.475	-119.50	419.36	18.38
Funicular 2 (Figure 12)	0.019	-119.50	266.69	70.29
Catenary (Figure 13)	**0.688**	-119.50	452.18	16.37
Fan-like (Figure 14)	0.008	-119.50	**258.36**	**99.58**
Truss (Figure 15)	0.019	-119.50	374.10	62.89

4.2.3 Load paths

The results of equations (5) and (6) are given in the second and third column of Table 2 respectively. Equation (5) is also verified for all the models, as *T-C* remains constant. For equation (6), the minimal value of *T+C* will be reached for the optimal load path of the fan-like network.

4.2.4 Stiffness considerations

The obtained values, set out in the last column of Table 2, show that the fan-like network is the stiffest. Force F considered is the total applied load, the magnitude of which is 1.195 [MN]. Stiffness is obtained for steel ties dimensioned to support a maximum effort of 2 [MN], as in concrete. This corresponds to a rebar section of 48.06 [cm²].

4.2.5 Comparison of results (Table 2)

A classification of networks according to their respective performance shows that results obtained for load paths and stiffness analyses are always correlated. The fan-like network is the lightest and the stiffest, followed by the second funicular one, the truss, the first funicular one, and finally the catenary. However, for this study case, these results do not converge with areas of admissible geometrical domains. So this means that among the sets of structural behaviour which can possibly be activated in the structure, the most efficient is not always the safer and most sufficient one considering robustness. Therefore, robustness properties have to be designed specifically by implementing alternative structural mechanisms characterised by larger geometrical domains.

5 Conclusion and perspectives

This paper presents a geometrical approach completing the existing numerical ones. It helps designing features linked to structural robustness, such as the position of rebars in concrete walls. The admissible geometrical domain as a proposed robustness indicator does indeed give information about possible force redistributions inside the structural shape and material. The analysis of two case studies establishes admissible geometrical domains for various networks of internal forces.

In so far as there exists an infinity of possible strut-and-tie networks in a concrete shear wall, the approach based on load paths reveals itself to be convenient for choosing the "right" strut-and-tie networks to implement. But as results do not guarantee that the optimal load path is robust enough, admissible geometrical domains can be checked in order to ensure minimal force redistributions and hence robustness.

Although the proposed geometrical approach is based on simplifying assumptions and presents some limitations - which makes no exception to the numerical approaches proposed in the relevant literature -, it allows qualitative comparisons that help taking robustness features into account at the very first step of the building process.

6 References

[1] Knoll F., Vogel T. *Design for robustness*. Structural Engineering Documents 11, International Association for Bridge and Structural Engineering. Zurich; 2009.

[2] *EN 1990* Eurocode: basis of structural design.

[3] *EN 1991-1-7* Eurocode 1: actions on structures, part 1-7: general actions - accidental actions.

[4] Cavaco E., Casas J.R., Neves L. Quantifying redundancy and robustness of structures. *International Association for Bridge and Structural Engineering report*. 2013; **100**: 78-99.

[5] Val D.V., Val E.G. Robustness of frame structures. *Structural Engineering International*. 2006; **16**(2): 108-112.

[6] Baker J.W., Schubert M., Faber M.H. On the assessment of robustness. *Journal of Structural Safety*. 2008; **30**(3): 253-267.

[7] Frangopol D.M., Curley J.P. Effects of damage and redundancy on structural reliability. *Journal of Structural Engineering*. 1987; **113**(7): 1533-1549.

[8] Smith J.W. Structural robustness analysis and the fast fracture analogy. *Structural Engineering International*. 2006; **16**(2): 118-123.

[9] Zastavni D., Deschuyteneer A., Fivet C. Admissible geometrical domains and graphic statics to evaluate constitutive elements of structural robustness. *International Journal of Space* Structures. 2016; **31**(2-4): 165-176.

[10] Maxwell J.C. On reciprocal figures and diagrams of forces. *Philosophical Magazine*. 1864; **4**(27): 250-261.

[11] Zalewski W., Allen E., Iano J. *Shaping structures: Statics*. New York: John Wiley and Sons; 1998.

[12] Fivet C. *Constraint-Based Graphic Statics, a geometrical support for computer-aided structural equilibrium design*. PhD thesis, Université catholique de Louvain; 2013.

[13] Schlaich J., Schäfer K., Jennewein M. Toward a consistent design of structural concrete. *PCI Journal*. 1987; **32**(3): 74-150.

[14] http://i-concrete.epfl.ch/applets/applets-1-01_f.asp

[15] Baker W.F., Beghini A., Mazurek A. Applications of structural optimization in architectural design. *Proceedings of the ASCE structures congress*. 2012.